

https://dspace.org/

Methods for condition monitoring and fault diagnosis on a synchronous 2 pole generator

Doorsamy, Wesley

2013-07-15
http://hdl.handle.net/10539/12829

Downloaded from a DSpace repository. https://dspace.org/

METHODS FOR CONDITION MONITORING AND FAULT DIAGNOSIS ON A SYNCHRONOUS 2 POLE GENERATOR

Wesley Doorsamy

A research report submitted to the Faculty of Engineering and the Built Environment, University of the Witwatersrand, Johannesburg, in fulfilment of the requirements for the degree of Master of Science in Engineering.

University of the Witwatersrand, Johannesburg, 2012

Declaration

I declare that this dissertation is my own, unaided work, other than where specifically acknowledged. It is being submitted for the degree of Master of Science in Engineering (MSc 50/50) in the University of the Witwatersrand, Johannesburg. It has not been submitted before for any degree or examination in any other university.

Signed this _____ day of _____ 20 _____

_____

Wesley Doorsamy

Abstract

In order to increase the integrity of existing generation systems, it is essential to discover problems well in advance. An investigation into methods for diagnosing multiple incipient faults on a 2-pole synchronous generator is presented. Simulation of the generator on a finite element analysis (FEA) software package is used to predict the effects of these faults. Experimental analysis of the generator under fault conditions is then conducted and confirms the predicted behaviour. The investigation utilises search coils and shaft brushes as condition monitoring tools. Results of the investigation indicate definitive relationships between the faults and specific harmonics of the output signals from the condition monitoring tools. The presented techniques are viable and future work can utilise these results in the design of a fault diagnosis system.

To my everything, Lorinda,

and,

the loving memory of my dear sister, Mandy.

Acknowlegements

I hereby acknowledge the National Research Foundation of South Africa for their financial support. Thanks to my project supervisor, Prof. Willie Cronje for his patience and guidance. Finally, thanks to the staff at the School of Electrical and Information engineering.

Contents

List of Figures **vii**

List of Tables **ix**

1 Introduction **1**
1.1 General . . . 2
1.2 Research Objectives . . . 3
1.3 Dissertation Layout . . . 3

2 Background **5**
2.1 Synchronous Generator Fundamentals . . . 6
2.2 Project Background . . . 8
2.3 Incipient Faults . . . 10

3 Experimental Layout **11**
3.1 Synchronous Generator . . . 12
3.2 Measurement System . . . 13
3.3 ControlDesk and Matlab Real-Time Interface . . . 16

4 Finite Element Analysis **17**
4.1 FEA Fundamentals . . . 18
4.2 Construction of Model . . . 19
4.2.1 Geometry . . . 19
4.2.2 Circuit and Coupling Components . . . 21
4.3 Modelling of Fault Conditions . . . 22
4.3.1 Rectifier Fault . . . 22
4.3.2 Eccentricity . . . 23
4.3.3 Short-circuited Excitation Windings . . . 24

5 Mini-gen Fault Conditioning **25**
5.1 Rectifier Fault . . . 26
5.2 Eccentricity . . . 26

5.3 Short-circuited Windings 28

6 Simulation and Experimental Results **30**
6.1 Signal Processing 31
6.2 Rectifier Fault 32
6.3 Eccentricity 34
6.4 Short-circuited Excitation Windings 35
6.5 Discussion 37

7 Conclusion **38**
7.1 Outcomes 39
7.2 Recommendations for Future Research 40

References **41**

A Simulation Model **44**
A.1 Material Characteristics 45

B Matlab Code **47**

C Instrumentation **49**
C.1 Current Probe 50
C.2 Peripherals 50

List of Figures

2.1 Cross-sectional front view of a cylindrical 2-pole synchronous generator . . 7
2.2 Flow diagram of fault diagnosis system for synchronous generator 9

3.1 Miniature generator and peripherals used in laboratory setup 12
3.2 Block diagram of experimental layout 14
3.3 Photograph of shaft brush arm riding on rotor shaft (left) and brush insert (right) used for measuring shaft voltages 15
3.4 Photograph of flux probe connector (left) and circuit diagram of anti-aliasing filter and protection circuit on connector (right) 15
3.5 Simulink® model of dSpace® input application created using the Matlab® Real-Time Interface Library 16

4.1 Cross section of 2-pole synchronous generator model constructed using Preflux® 2-D 20
4.2 Simulation equivalent model for 2-pole synchronous generator constructed using Preflux® 2-D 21
4.3 Translation of coordinate system for rotor relative to stator for initialisation of eccentricity fault condition in simulation model 23
4.4 Coil element on geometric model (left) and short-circuited coil element (right) in circuit model used to simulate short-circuited excitation windings 24

5.1 Three phase rectifier with single open-circuited diode for implementation of rectifier fault condition 26
5.2 Longitudinal cross-section (side-view) of mini-generator 27
5.3 Spacers used for adjustment of stator position relative to rotor for implementation of static eccentricity fault 27
5.4 Adjustment of stator position relative to rotor for introduction of static eccentricity fault 28
5.5 Mini-gen rotor during construction with concentric field windings 29
5.6 Short-circuiting of field windings through use of brass sheet metal on rotor winding overhangs 29

6.1 Frequency content of power spectral density of shaft voltage without fault . 33
6.2 Frequency content of power spectral density of shaft voltage with rectifier fault 33
6.3 Simulated rotor winding current under normal and rectifier fault conditions 34
6.4 Rotor winding current measurement of experimental setup under normal and rectifier fault conditions 34
6.5 Frequency content of power spectral density of shaft voltage with excitation winding fault 36

A.1 B-H curve of FLU_M400 steel used for stator core construction in Flux® 10.4.1 45
A.2 B-H curve of FLU_1010_XC10 steel used for rotor core and case construction in Flux® 10.4.1 45
A.3 Resisivity characterisitcs of FLU_copper used for all coil and damper construction in Flux® 10.4.1 46

C.1 Current probe used to measure three-phase rectifier output to field windings on rotor 50
C.2 Amplifier used with current probe to measure three-phase rectifier output to field windings on rotor 50
C.3 BNC termination (feedthrough) used to connect amplifier to DSpace controller panel 51
C.4 CLP1104 controller panel used to interface with dSpace card and workstation 51

List of Tables

6.1 Percentage change in harmonics of flux probe signal for rectifier fault . . . 32
6.2 Percentage change in harmonics of shaft voltage for rectifier fault 32
6.3 Percentage change in harmonics of flux probe for static eccentricity fault . 35
6.4 Percentage change in harmonics of shaft voltage for static eccentricity fault 35
6.5 Percentage change in harmonics of flux probe for excitation winding inter-turn short circuit fault 36
6.6 Percentage change in harmonics of shaft voltage for excitation winding inter-turn short circuit fault 36

Chapter 1

Introduction

1.1 General

With the growing energy demand globally, great emphasis has been placed on generating capacity and ability to meet projected load demands. This has prompted strict management of energy and new initiatives to alleviate stresses on power networks. Additionally, the ageing of conventional generator units has incited uncertainty with regards to reliability. Therefore it has become essential to manage excess generating capacity where possible and increase the integrity of current generation.

While the area of research with respect to alternative methods of generation of energy is vast and filled with possibility, it is necessary to effectively manage systems which currently form part of the incumbent infrastructure. This means placing a firm interest in ensuring the reliability of current systems and considering new methods in discovering incipient problems within these systems.

Currently, within these systems, the generator is probably the most significant module and because of the necessity for the paramount reliability of such generators it is imperative that problems are discovered well in advance.

There is a vast majority of condition monitoring techniques which utilise the advancement in digital processing equipment. The selection of condition monitoring systems is made somewhat difficult to due to cost, reliability and complexity. Components required for some condition monitoring systems can be quite expensive and still not diagnose incipient faults. Additionally, there is the problem of complexity with these systems as various instrumentation and intricate control techniques are required.

Scope of this work includes investigating and developing methods of diagnosing faults on generators. The research intends to deduce these methods through introducing specific faults and determining the effects thereof. It is with these methods that the ultimate objective of a more efficient, reliable and proactive system of condition monitoring may be realised.

1.2 Research Objectives

While there is some previous work in the area of fault diagnosis on synchronous generators, results are not nearly enough to develop a complete system which can utilise cost effective, reliable and uncomplicated methodologies to diagnose incipient faults. Past results indicate the possibilities of utilising shaft voltages for the purpose of diagnosing faults, however these results have not been quantified. Previous work, relevant to the scope of the presented research, is discussed in detail in Section 2.2.

The purpose of this research project is to examine the effects that a defined set of faults have on shaft brush and flux probe signals. Additionally, these effects are to be quantified and relationships with specific faults to be identified. The main objectives of the research is summarised as follows:

- Construction of a model of the generator using finite element analysis (FEA) software.
- Implementation and simulation of fault conditions.
- Measurement of shaft voltage and flux probe signals under normal and fault conditions, with the generator under no-load and load conditions.
- Analysis of simulation and measurement data using suitable signal processing techniques.
- Validation of hypothesis through characterisation of distinct relationships between faults and effects on the signals.

1.3 Dissertation Layout

- **Background** - Chapter 2 firstly presents fundamental theory of a synchronous generator as this relates to the machine utilised in the investigation. A summary of some previous work on fault diagnosis is then given followed by a detailed description of the project background.

- **Experimental Layout** - Chapter 3 deals with the experimental layout used i.e. synchronous generator, induction motor, instrumentation and data capturing equipment. A detailed description of each component of the experimental investigation is presented.

- **Finite Element Analysis** - Chapter 4 presents the FEA/simulation portion of the project. An in-depth analysis of the model constructed using Flux® 10.4.1 and simulation of fault conditions is included. Additionally, the significance of the simulations in prediction of actual behaviour of the machine is discussed.

- **Mini-gen Fault Conditioning** - Chapter 5 examines how each of simulated fault conditions was implemented in the experimental system. This includes a rectifier fault, rotor eccentricity and short-circuited excitation windings.

- **Simulation and Experimental Results** - Chapter 6 gives results obtained from simulations and the experiment. The prediction result is compared with the actual behaviour and definitive relationships are obtained from this for the purpose of fault diagnosis.

- **Conclusion** - Finally, chapter 7 critiques the research outcomes and objectives. Recommendations for future investigations regarding overshadowing effects and an automated fault diagnosis system are then offered.

Chapter 2

Background

2.1 Synchronous Generator Fundamentals

Synchronous generators are commonly used, in a global context, for power generation schemes and the application of distributed generators and in a South African context, is dominated by schemes operating these machines [1]. Most electric energy is produced in rather constant-speed-regulated synchronous generators that deliver constant AC voltage into regional and national power systems, which is then transported and distributed to consumers. This is the case with fossil fuel, hydro and wind schemes that use mechanical energy in a turbine (prime mover) to drive the generators. Due to this widespread industrial utilisation of this specific machine, the presented research places particular focus on the synchronous generator (Section 3.1).

As mentioned special interest is given to synchronous generators commonly found in power stations i.e. large turbo-generators. These generators are characterised by a uniformly slotted stator laminated core that hosts 3-phase windings and DC current excited non-salient (cylindrical) rotor (see Figure 2.1) With these generators, the speed (n) is rigidly bound to the stator frequency (f), as indicated in the following equation:

$$n = \frac{60 \times f}{p} \tag{2.1}$$

Where n is the rotor speed in rpm
f is the stator frequency in Hz
p is the number of pole pairs

Therefore, using Equation 2.1 with a frequency of 50 Hz and a single pole pair (DC), the speed is given as 3000 rpm. Due to these high speeds, it is necessary, especially in large turbo generators, to protect the DC excitation coils against high centrifugal forces with rings of highly resilient resin materials. The sinusoidal air gap field distribution is accomplished and consequently there is a reduced harmonic content in the induced voltages on the stator.

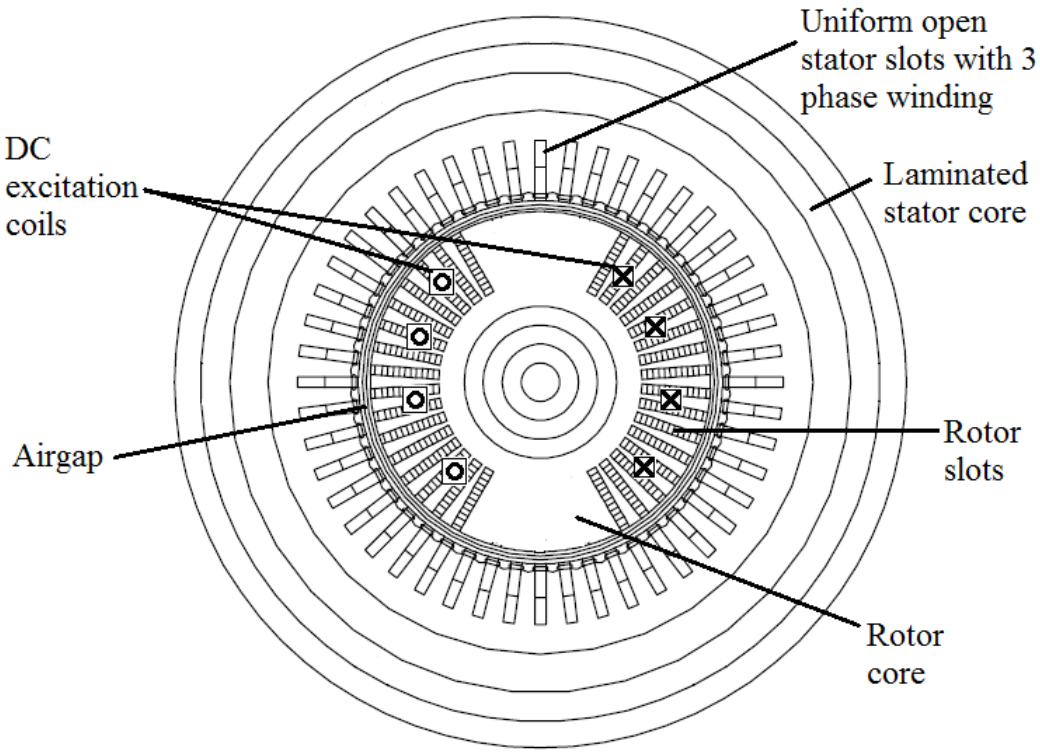


Figure 2.1: Cross-sectional front view of a cylindrical 2-pole synchronous generator

The rotor body is made from solid bar for better rigidity and heat transmission. Stator slots in large synchronous generators are open and are sometimes provide with magnetic wedges to reduce the content of electromagnetic force harmonics and additional losses in the rotor damper cage. When running at synchronous speed, at steady state, it is expected that the rotor damper cage currents are zero. Ideally, this neglects the stator magnetomotive force space harmonics due to the placement of windings in slots, due to slot openings and other imperfections. However, in real machines, space harmonics induce voltages and thus produce eddy currents in the rotor damper cage, even during steady state [2].

2.2 Project Background

Research has been conducted on the use of shaft signals as a method for condition monitoring and diagnosing faults in synchronous generators. This area of research has been successful specifically with regards to diagnosis of eccentricity [3, 4]. Eccentricity of a rotor can lead to system vibration, bearing failure and even thermal bending of the rotor due to asymmetrical magnetic fields. Common indicators used to diagnosis these faults are bearing vibrations and torsional oscillations of the shaft. The use of the aforementioned mechanical symptoms has been found to be insufficient as the fault has already developed into multiple faults and possibly caused considerable damage to the machine. Measurement and analysis of shaft currents and voltages have been investigated to provide an alternative method to diagnosing faults incipiently, hence preventing considerable damage.

Shaft voltages and currents have been found to cause problems such as bearing and seal deterioration, and as a result many methods have been proposed to attenuate these signals [5]. These signals are practically unavoidable due to a number of reasons based on points of origin. Shaft voltages and currents are caused by a number of reasons including magnetic asymmetries due to imperfections in the machine manufacture and faults such as rotor eccentricity [4, 6].

Winding faults also tend to occur due to insulation failure as a result of intense centrifugal forces in the case of rotor windings. Short-circuited windings pose the problem that a single short-circuited turn does not immediately indicate any problems, however localised heating can occur leading to further degradation of insulation and eventually more shorted turns. It generally takes a long time for a generator to return to a healthy operational mode from the winding faults and a early fault detection system is inevitably required to prevent downtime and high maintenance cost.

Diagnosis of faults such as eccentricity has been widely examined for machines such as induction motors [7]. Also, many techniques for condition monitoring involve the use of

chemical (insulation and bearing oil analysis) and mechanical (vibration, speed and temperature monitoring) methods[8]. Most of these methods involve use of off-line methods and rely on diagnosing faults through symptoms of damage/deterioration.

Early detection of faults assists in preventing unplanned maintenance due to damage or deterioration and in some cases, catastrophic failure [9, 10]. Deliberation of methods utilising on-line monitoring that ensures diagnosis of incipient faults is relatively unsubstantial. Furthermore, these methods have also been restricted to diagnosis of single faults at a time.

The purpose of this project is to verify some of these methods of condition monitoring not only to identify, but to quantify the faults also. Characterisation of the relationship between faults and signals (flux probe and shaft brushes) shall enable the conception of a real-time on-line condition monitoring system (shown in Figure 2.2). Such a system shall provide an appropriate response i.e. log, alarm, trip, when a fault is detected and diagnosed.

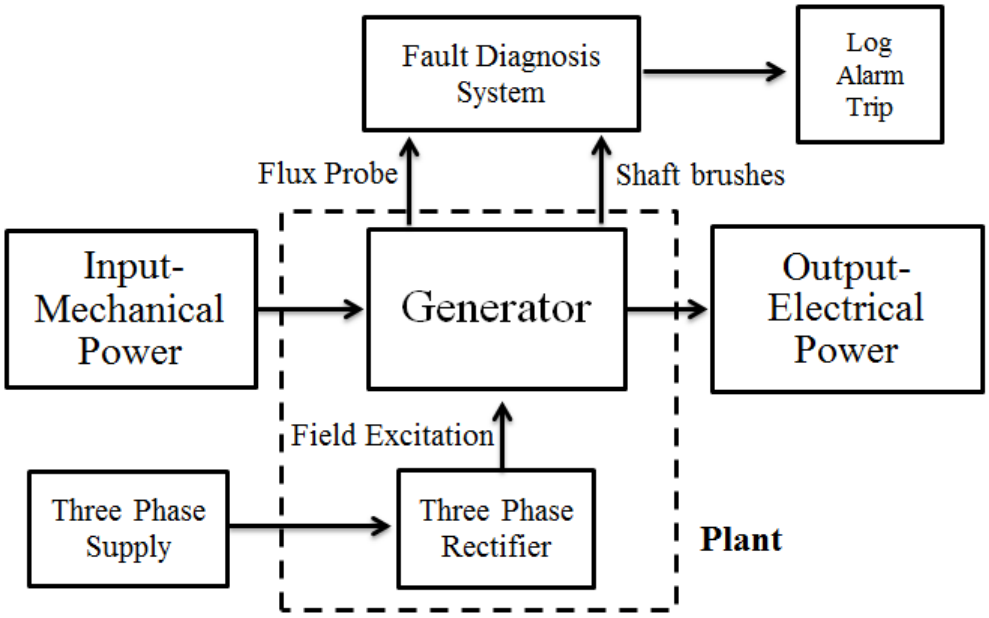


Figure 2.2: Flow diagram of fault diagnosis system for synchronous generator

2.3 Incipient Faults

In application, generators consist of numerous interconnected systems (accessories/peripherals) such the prime mover, excitation systems etc. which influence the performance of the generator. The extent of the research being conducted is limited to the scope of the actual generator. However, interest is placed on the excitation system (three phase rectifier) as faults within this system influences performance of the machine.

Evaluation of various faults with respect to the tendency of the fault to further develop, immediate effects, long-term effects and overall system influence, has prompted focus in excitation winding, rectifier and static eccentricity faults.

A rotor winding short circuit occurs as a typical machine failure that can lead to further short-circuited turns and localised heating. Unbalanced forces due to the inherent asymmetrical flux can also result in rotor vibrations [11, 12, 13].

Rectifier faults are easily detectable when two or more diodes are destroyed, resulting in a substantial drop in the excitation current. A single defective diode results in a moderate drop in the excitation current and is therefore not as easily detected. Additionally, industrial units are also fitted with automatic voltage regulators (AVRs) to regulate excitation levels.

Shaft eccentricity can also lead to vibration due to the displaced air-gap and resulting asymmetrical forces. Early detection of rotor eccentricity is significant as further development of this fault can result in damage to windings, stator core and rotor core [14]. Diagnosis of these faults is especially significant during continuous operation, therefore the methods presented are applicable under steady-state conditions. Effects of each fault on specific harmonics are of primary interest as this will allow for the conception of a definitive method to differentiate between faults under combinational fault conditions.

Chapter 3

Experimental Layout

3.1 Synchronous Generator

The experimental configuration consists of a miniature generator (hereafter also referred to as a mini-gen), specifically designed to mimic large turbo-generators. The miniature generator is a 20 kVa, 2-pole, 3000 RPM, 50 Hz machine which is intended to imitate the operation of a 660 MW turbo-generator with solid cylindrical rotor core, open stator slots and insulated bearings. Although the investigation into methods for faults diagnosis is specific to a synchronous generator, it is not conceptually exclusive to this machine.

Figure 3.1 shows the laboratory setup. The setup uses a 3 phase induction motor (prime mover) to drive the mini-gen. The three phase rectifier inputs a 3 phase AC voltage and supplies the slip rings with DC for field excitation.

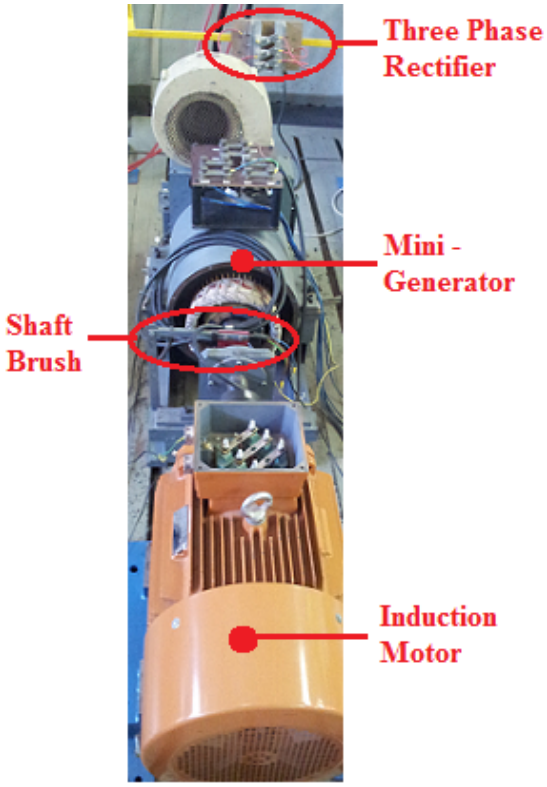


Figure 3.1: Miniature generator and peripherals used in laboratory setup

Large turbo generators are unlike commercially available generators which typically have four or more poles. Additionally, the miniature generator has the similarity to large turbo-generators in that the rotor has been machined from solid bar and consists of concentric distributed field windings.

The generator has been designed to accommodate various fault conditions and measurements of resulting conditions. Some of these capabilities include:

- Adjustable stator in order to change positioning relative to rotor thereby introducing eccentricity.
- DC excitation system via slip rings made accessible.
- Shaft brushes to enable measurement and grounding.
- Flux probes in the form of thin copper wires placed in stator slots, wrapped around teeth.
- Each stator coil end is accessible for measurement and stator (mush wound) overhangs are accessible to allow fault introduction.

3.2 Measurement System

The measurement system (see Figure 3.2) consists of a data acquisition system which utilises Matlab® and dSpace® software. The dSpace system consists of a 'break-out box' or controller panel (CLP1104) that consists of Analogue-to-Digital converters (ADC) and Digital-to-Analogue converters (DAC). Various outputs from the generator, e.g. Current Transformers (CT) on the stator coils' ends (before phase outputs), are connected to the ADC ports of the CLP1104 controller panel. The controller panel communicates with a computer via a dSpace interface card (DS1104 R&D Board) (see Appendix C).

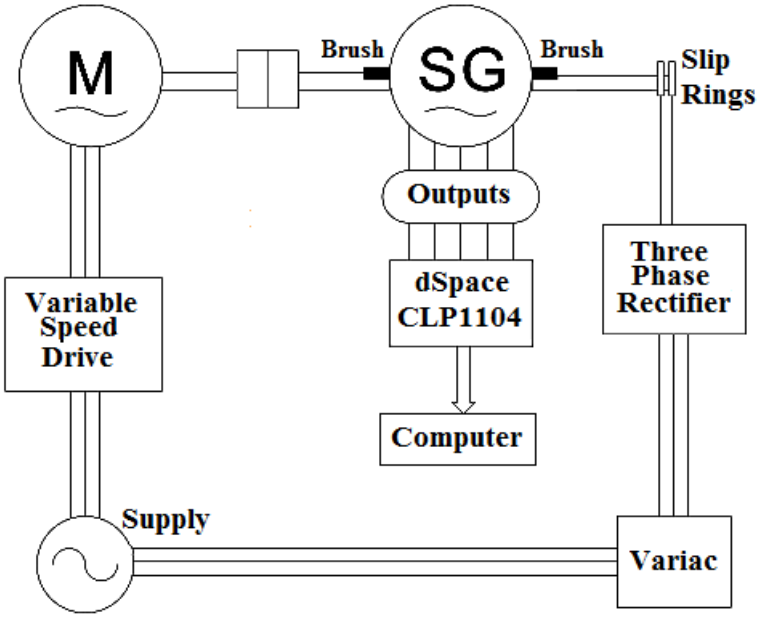


Figure 3.2: Block diagram of experimental layout

Matlab consists of embedded dSpace systems that enable the user to interact with the controller board and interconnected devices. This interaction is accomplished through use of Simulink® models available from the dSpace library. Once the model is built and the program loaded onto the controller board, ControlDesk® (dSpace software) allows data to be captured and processed in real-time. This implies that condition monitoring may be done in real-time and is therefore on-line monitoring.

A significant component of the measurement system is the instrumentation. Specialised silver-gold brushes are used and are placed on the finished landings on either side of the mini-gen rotor shaft. The brushes are connected to the ADC inputs of the dSpace controller panel and allows for measurement of induced voltages across the shaft. Figure 3.3 shows a brush arm with the brush riding the rotor shaft.

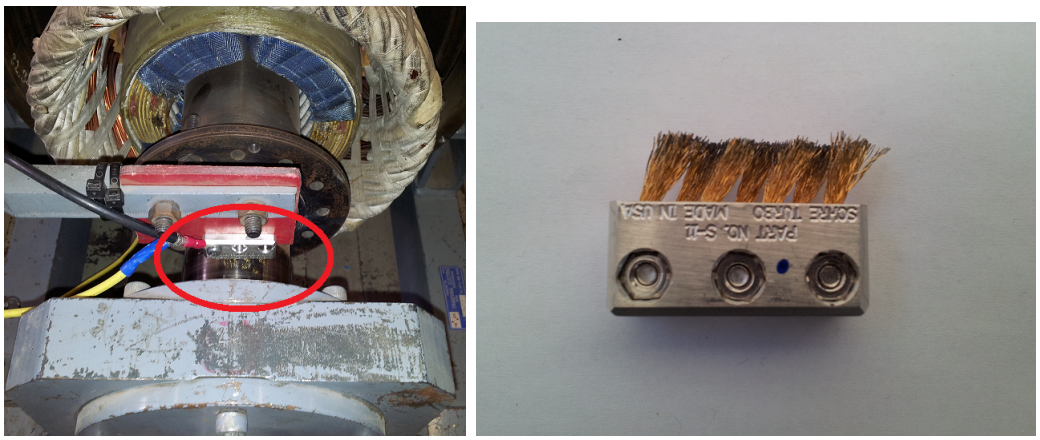


Figure 3.3: Photograph of shaft brush arm riding on rotor shaft (left) and brush insert (right) used for measuring shaft voltages

In addition to the brushes, flux probes/search coils are used to measure the magnetic perturbations within the machine. The flux probe comprises of a single turn copper conductor which runs through a stator slot, along the length of the stator, and loops around the stator tooth. These flux probes are positioned all around the stator at 30° intervals. Each of the probes' outputs are fitted with a fuse, anti-aliasing filter and connector (see Figure 3.4). Similarly, as with the brushes, the probes are connected to the ADC inputs of the dSpace controller panel.

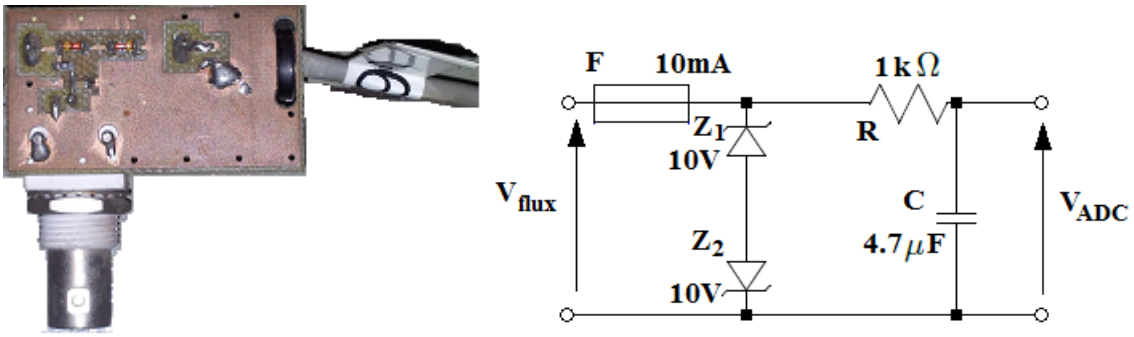


Figure 3.4: Photograph of flux probe connector (left) and circuit diagram of anti-aliasing filter and protection circuit on connector (right)

3.3 ControlDesk and Matlab Real-Time Interface

ControlDesk is dSpace's user-interface software and provides functions to control, monitor and automate experiments [15]. The software consists of various integrated managers which perform these functions such interfacing with the platform i.e. Simulink and DS1104 board, and handling experimental data.

In order to carry out the required signal measurements on the mini-gen, complete configuration of the platform, interface and application is necessary. Firstly, the Matlab real-time interface library is used to create a model in Simulink (see Figure 3.5). The model is then built and loaded onto the DS1104 board.

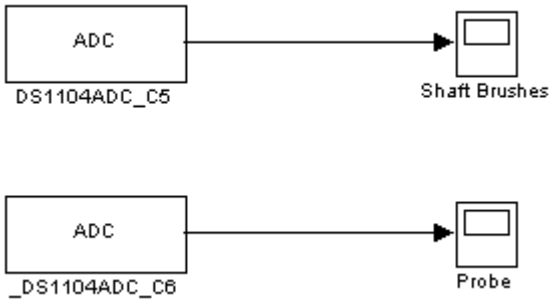


Figure 3.5: Simulink® model of dSpace® input application created using the Matlab® Real-Time Interface Library

When the application is built, a new variable sequence is created and allows for an experiment to be created in Controldesk® (dSpace). The new experiment created uses these variables together with a specifically designed layout, consisting of virtual instrumentation, to monitor and record each of the signals in real-time.

Chapter 4

Finite Element Analysis

4.1 FEA Fundamentals

The evolution of the Finite Element Method (FEM) is closely connected with the development of engineering and computer sciences. Variational methods of FEM in electromagnetics require numerical procedures established through functionals. The investigated system i.e. synchronous generator, essentially fits into a classical 2-D case with usual functionals and is therefore simplified through geometric characterisation such as periodicity. However, with implementation of faults such short-circuited windings and eccentricity, the complete 2-D case of the generator is required.

Model complexity is introduced through the addition of electronic devices such as the three-phase rectifier, flux probe etc. This problem is usually solved through simulating coupling between electronic circuits/devices and consists of determining the fluxes and winding inductances for performing calculations based on lumped parameters representing the magnetic part of the set [16].

Fundamentally, finite element analysis uses mathematical methods for solving ordinary and partial differential equations [17]. The software utilised for the construction of the model does not require the user to have a comprehensive knowledge of the aforementioned functionals or derivations thereof (Maxwell's equations). Only specific details pertaining to the problem are required together with completion of certain tasks such as creation of geometry, selection of boundary conditions, creation of coupling circuit, definition of mesh and selection of solver.

Some assumptions are inherently made with the selection of a 2-D model such as the direction of the magnetic fields and flow of currents. Additionally, it is assumed that the stator and rotor are of equal length. However, the package is believed to be suitable for the purpose of this investigation as an axisymmetric model is adequate for implementation of all the concerned faults.

4.2 Construction of Model

A model of the synchronous generator was constructed using Flux® 10.4.1, developed by Cedrat. The construction of the model consists of three principle stages:

- Definition of geometrical parameters and construction of 2-D model.
- Definition of physical parameters such as regions, materials etc.
- Construction of electric circuit model.
- Meshing of study domain and solving of problem.

4.2.1 Geometry

The data and characteristics of the generator, given in 3.1, are used to construct the geometrical model. Firstly, the coordinate systems are defined. Separate coordinate systems are adopted for the rotor and stator, in order to allow for eccentricity to be modelled at a later stage. Three geometric entities are used to construct the entire model i.e. points, lines and arcs. The stator and rotor core laminations are defined using points and arcs.

One of the design features included in the Preflux® software is a user-defined geometrical transformation function. It is only necessary to create and completely define a single slot of the stator and rotor, as transformation functions are then created to define every other slot with relation to another previously defined slot. Two main transformation functions are utilised i.e. one which rotates a new slot by a predefined angle and one to mirror each slot thereby creating the second stator/rotor half. Figure 4.1 shows the complete geometrical model of the generator.

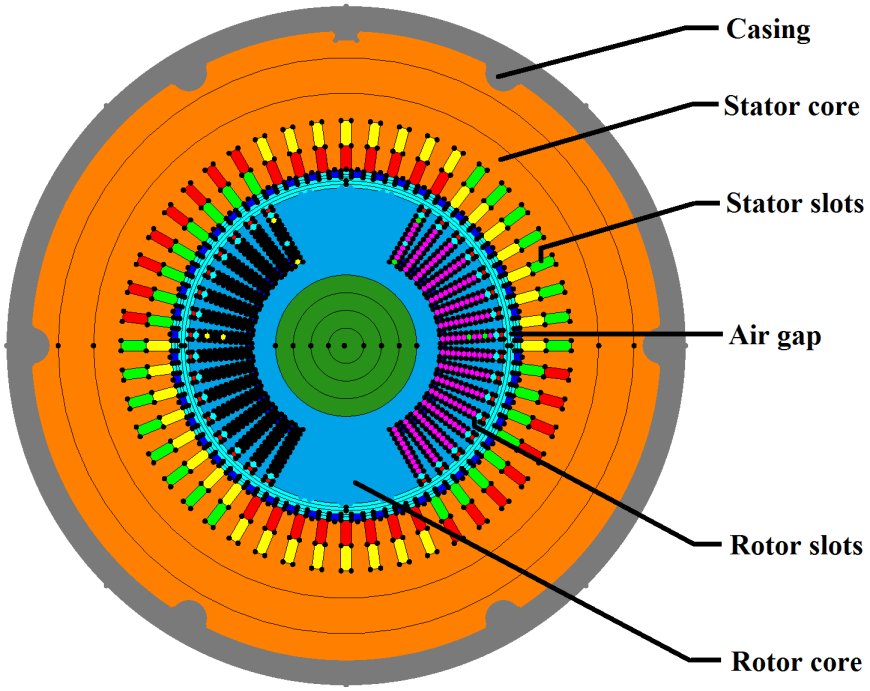


Figure 4.1: Cross section of 2-pole synchronous generator model constructed using Preflux® 2-D

The model of the generator is specifically constructed to mimic the actual generator and includes the following features:

- FLU_STEEL_1010_XC10 casing with weld recesses on casing around stator
- M400_STEEL laminated stator core with 48 slots
- Stator coils per phase with slot allocated to each coil per direction
- FLU_STEEL_1010_XC10 2-pole rotor core
- 32 rotor slots with 16 slots per side
- 6 mm Air gap
- 38 copper dampers around shaft

These features or elements are defined as face regions in the physics of the model. Characterisation of each region is completed through associating each element with a coupling

component constructed with the circuit editor. Materials selected are part of the standard library and characterstics of each of the materials used are given in Appendix A.

This electrical circuit forms part of the physics and is therefore essential to the model. The circuit consists of magnetic coupling components and electrical components. Hence, the cores, windings and any external electrical components are essentially defined using the circuit editor.

4.2.2 Circuit and Coupling Components

In addition to the presented geometrical component, the simulation model also includes a physics component. The physics of the simulation model characterises the various elements of the geometry through a coupling/ circuit model. For example, the stator slots are represented by coil conductors with specific thickness, resistance etc. The coupling circuit comprises of not only the electrical components but magnetic components as well and is therefore not exactly an electrical circuit. The model is shown in Figure 4.2.

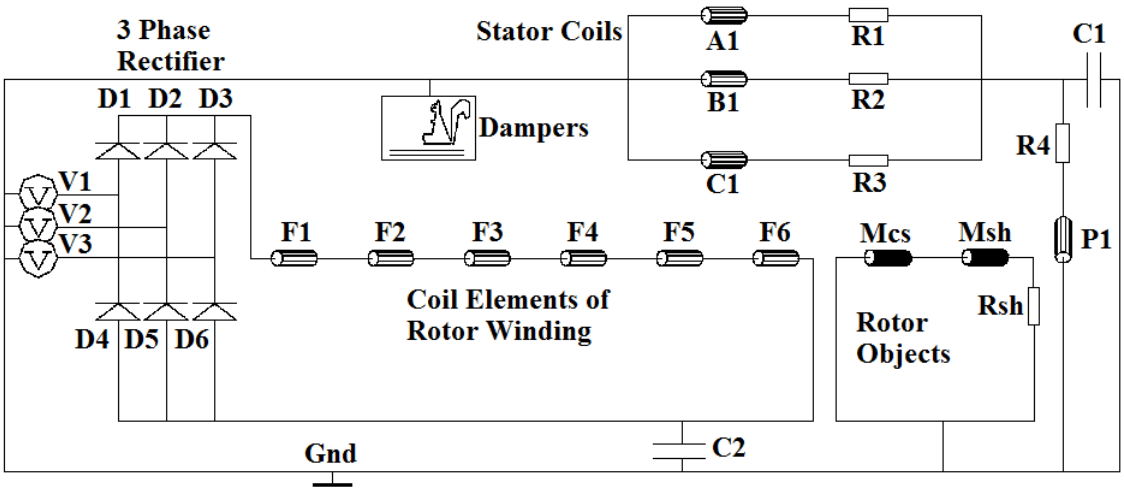


Figure 4.2: Simulation equivalent model for 2-pole synchronous generator constructed using Preflux® 2-D

The sources V1, V2 and V3 constitute the three phase supply to the rectifier (represented by diodes D1 - D6). The output of the rectifier provides DC for the field excitation and is

therefore in series with the rotor windings. The stranded coil conductors F1-F6 characterise the field windings. Coil elements A1, B1 and C1 represent each of the stator coils. Steel components of the machine are also included this model and are represented as the stator case (Mcs) and rotor shaft (Msh). Resisitor Rsh represents the shaft resistance and coil conductor P1 acts as the flux probe/ search coil. Capacitor C1 and resistor R4 act form the low pass filter circuit. This filter mimics the effects of the flux probe connector shown in Figure 3.4.

Each of the previously described faults are implemented on the model and each scenario is simulated individually. The flux probe is modelled using a coil conductor (P1) which runs along the length of the machine, around the stator tooth (at various angular positions) and returns along the machine in the opposite direction. Shaft voltage measurements are performed directly across the shaft resistance (Rsh) of the circuit model and simulate the shaft riding brush measurements.

4.3 Modelling of Fault Conditions

In order to mimic the relevant fault conditions with the simulation model, specific circuit elements and geometrical features are manipulated. A description of the initialisation of each fault condition is presented in the following subsections.

4.3.1 Rectifier Fault

The three-phase rectifier is essential in providing a stable DC supply for the field windings. A single diode fault, essentially an open-circuited diode, results in a slight drop in the stator output voltages and is remedied, in industrial units, through use of an Automatic Voltage Regulator (AVR). This regulator tends to apply appropriate control to the excitation voltage, usually by increasing the supply to the rectifier. A single diode fault is therefore seen as an incipient fault as the resulting drop in excitation current is as easily detectable as two or more diode faults.

Simulation of this fault scenario is carried out by simply removing a single diode e.g. D1, of the coupling model (as shown in Figure 4.2). A complete three-phase rectifier circuit was initially constructed, instead of a simple current source, precisely for this purpose.

4.3.2 Eccentricity

Different degrees of eccentricity may occur in various machines, however the fault exhibits tendency to further develop. Minor cases of rotor eccentricity .i.e. small deviations symmetry, is initialised within the model as the investigation specifically focuses on incipient faults.

During the construction of the geometric model, separate coordinate systems were created for the rotor and stator. The points of origin for both coordinate systems are the same i.e. (0 ; 0) under normal conditions. Since each geometric element (point, line and arc) is defined with respect to the rotor coordinate system, eccentricity is introduced through shifting entire the rotor coordinate system. It is possible to achieve various levels of asymmetry through varying the coordinate systems and therefore shifting the rotor completely.

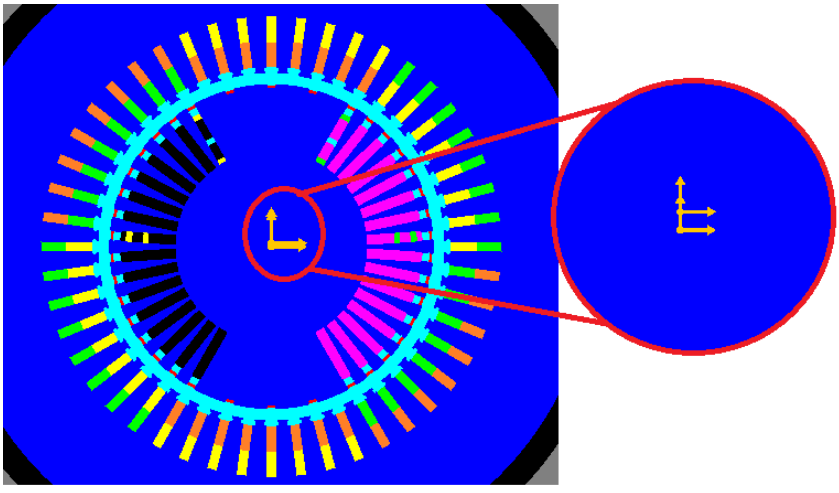


Figure 4.3: Translation of coordinate system for rotor relative to stator for initialisation of eccentricity fault condition in simulation model

4.3.3 Short-circuited Excitation Windings

Field windings on the rotor are highly susceptible to damage and deterioration. Large centrifugal forces and localised heating contribute to short-circuited windings on the rotor. This fault also has a tendency to further develop and is included in the investigation as detection is difficult, especially during early stages.

In order to mimic the fault condition, coil elements are distributed on the rotor in the geometric model. The corresponding coil elements are represented by coupling conductors within the circuit model. The fault condition is therefore initialised through short-circuiting a coil conductor in the circuit corresponding to the appropriate coil element in the geometric model. This is illustrated in Figure 4.4 with an example of a single-turn short circuit on the rotor winding.

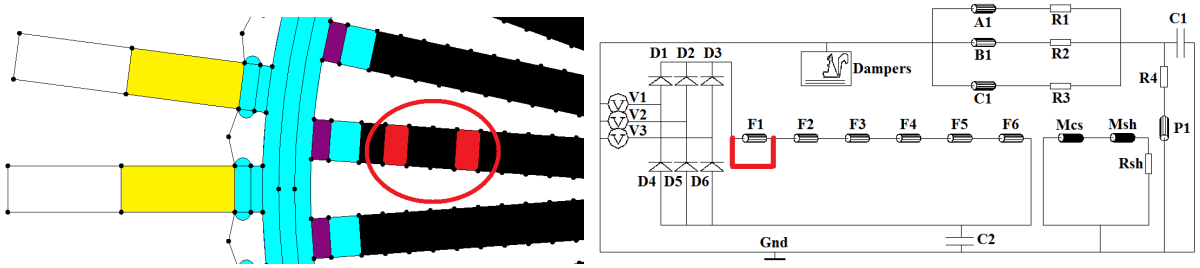


Figure 4.4: Coil element on geometric model (left) and short-circuited coil element (right) in circuit model used to simulate short-circuited excitation windings

Chapter 5

Mini-gen Fault Conditioning

5.1 Rectifier Fault

The first fault to be experimentally introduced is a three-phase rectifier fault. As previously described, the significance in investigating this condition originates from the difficulty in diagnosing the fault. This diagnosis is especially difficult with industrial units fitted with regulators (AVRs) when a single diode is defective.

A three-phase rectifier, comprising of 6 diodes, is supplied with variable three-phase voltage (variac). Outboard slip-rings are used to excite the rotor field windings with the output from the rectifier. The fault is implemented by simply open-circuiting a single diode i.e. removing the diode from the rectifier bridge circuit as shown in Figure 5.1.

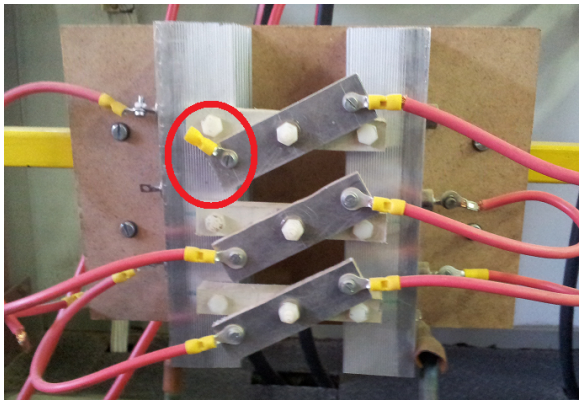


Figure 5.1: Three phase rectifier with single open-circuited diode for implementation of rectifier fault condition

5.2 Eccentricity

Capabilities of the mini-gen include an adjustable stator and this is used to alter the position of the stator relative to the rotor. The rotor is fixed on bearing pedestals and the winged-stator core is seated on the machine foundation/bedplate, as shown in Figure 5.2. It is therefore possible to alter the position of the stator along the vertical axis and horizontal axis.

Eccentricity is effectively introduced through raising the stator along the vertical axis and displacing the air-gap so that the rotor is positioned closer to the lower half of the stator. This is accomplished through antagonistically fixing the bolts along each side and using spacers to lift the outer shell/ case of stator, as shown in Figure 5.3.

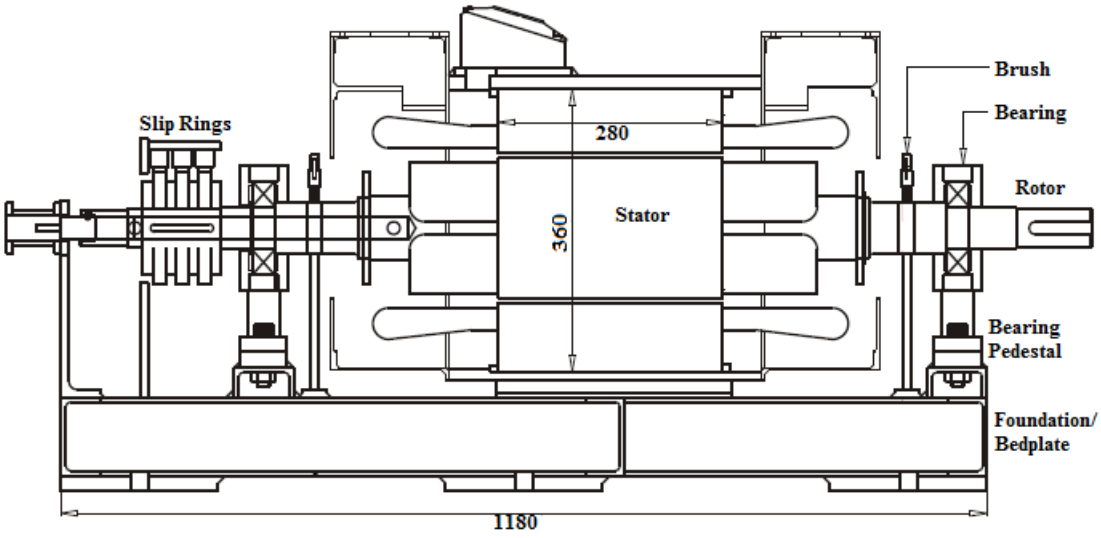


Figure 5.2: Longitudinal cross-section (side-view) of mini-generator

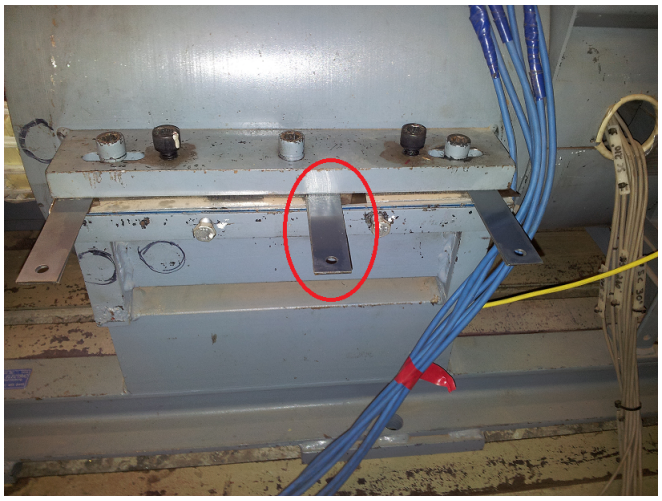


Figure 5.3: Spacers used for adjustment of stator position relative to rotor for implementation of static eccentricity fault

Through varying displacement δ (as indicated in Fig. 5.4), the rotor is displaced vertically from the centre axis by the same magnitude. It is therefore possible to introduce static eccentricity on the rotor through varying degrees. Eccentricity is varied to different levels experimentally to obtain a satisfactory indication of the change in relevant harmonics.

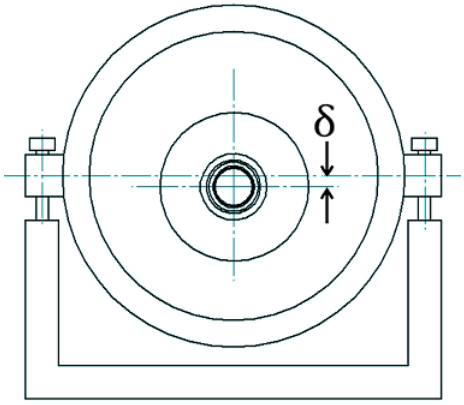


Figure 5.4: Adjustment of stator position relative to rotor for introduction of static eccentricity fault

5.3 Short-circuited Windings

Short-circuited field windings are also included as an incipient fault condition. Faults on rotor windings are often difficult to diagnose due to the inaccessibility of the problem area and is especially challenging with industrial units during continuous operation. Short-circuit faults on rotor windings may be caused through insulation failure and leads to localised heating. While a single turn short-circuit is not immediately noticeable, this fault has a tendency to develop and eventually result in significant damage.

The mini-gen rotor consists of distributed concentric field windings on the rotor. There are 32 slots machined onto the 2-pole rotor i.e. 16 per side, with 10 turns as shown in Figure 5.5. Rotor overhangs are readily accessible with each of the turns exposed. The short circuit fault is created through firstly shaving off winding insulation and then inserting brass sheet metal across 2 turns as indicated in Figure 5.6.

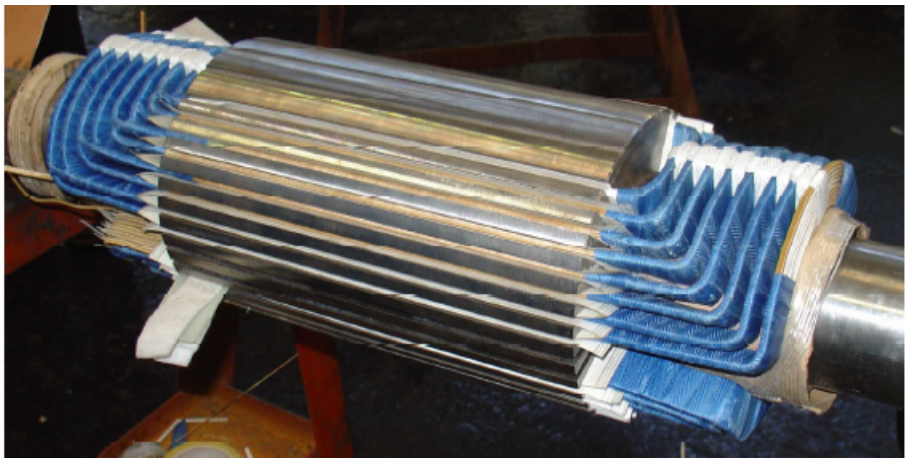


Figure 5.5: Mini-gen rotor during construction with concentric field windings

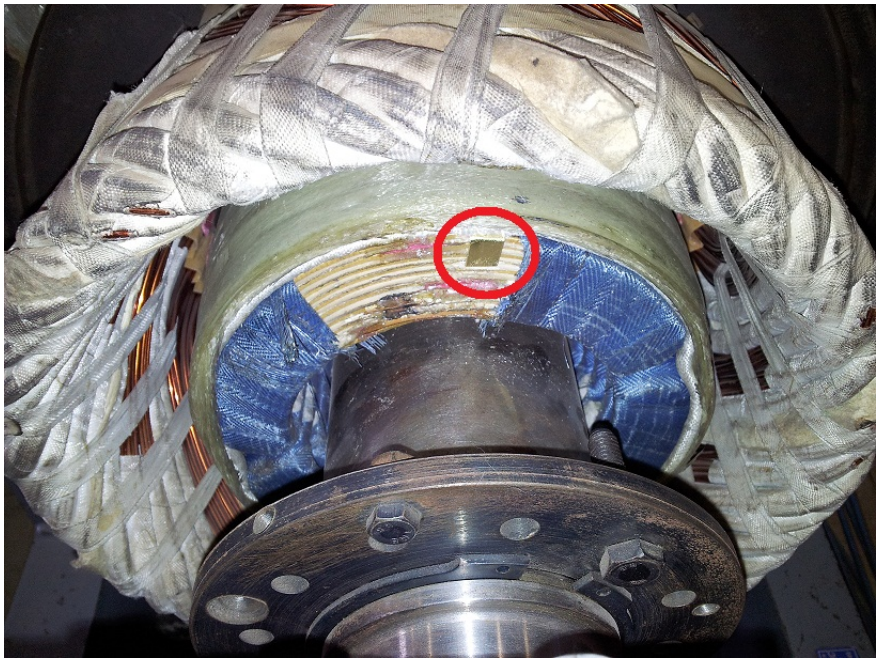


Figure 5.6: Short-circuiting of field windings through use of brass sheet metal on rotor winding overhangs

Chapter 6

Simulation and Experimental Results

6.1 Signal Processing

Both the simulation results and measured data require processing to ascertain usable information. An algorithm is implemented in Matlab® for this purpose. The algorithm inputs each of the signals, performs a Fast Fourier Transform (FFT) and compares power spectra of the signals obtained under fault conditions to normal conditions.

The frequency content of each signal is of principal interest and the power spectral density is used to obtain a more practical characterisation of each signal. The power spectral density describes how the power of the signal is distributed in frequency spectrum [18]. The method used to obtain the power spectral density (PSD) of the resulting signals consists of the derivation of the PSD for the discrete signal. This is accomplished through first using the definition for the PSD function and Fourier transform (continuous-time).

$$P_f = \frac{1}{2\pi} \int_{-\infty}^{\infty} \lim_{T \to \infty} \frac{1}{T} |X(\omega)|^2 \tag{6.1}$$

Where the Fourier transform of function $x(t)$ is given as

$$X(\omega) = \frac{1}{2\pi} \int_{-\infty}^{\infty} x(t)\, e^{-i\omega t} dt \tag{6.2}$$

However, the resultant signal is sampled at discrete times with N number of samples for a total measuring period of T and may be expressed as the finite time-series given in Equation 6.3.

$$x_n = x(n)dt \tag{6.3}$$

Where n is the sample number and
dt is the sampling period

Hence, by normalising the power spectral density function i.e. for the total sample period T and using the Discrete Fourier Transform (DFT) of the time series, the power spectral density of the measured signal, in V^2/Hz, may be expressed as

$$P_n = \frac{dt^2}{T} \sum_{n=1}^{N} x_n e^{-i2\pi fn} \tag{6.4}$$

From this output, the percentage differences in the relevant harmonics are acquired. Only the considerably affected harmonics, under each fault condition, are significant to the objective of establishing a relationship between the fault and affected frequencies.

6.2 Rectifier Fault

Using the aforementioned methods for processing the signals, the change in the frequency content of the flux probe and shaft signals from normal to fault conditions is extracted. Harmonics that are affected by a rectifier fault are indicated in Table 6.1 and Table 6.2.

Table 6.1: Percentage change in harmonics of flux probe signal for rectifier fault

Condition	Harmonic (Hz)	Simulation	Measurement
		Percentage change (%)	
No Load	200	39.31	1129.74
	250	63.18	90.07
Full Load	200	24.43	808.86
	250	62.82	64.95

Table 6.2: Percentage change in harmonics of shaft voltage for rectifier fault

Condition	Harmonic (Hz)	Simulation	Measurement
		Percentage change (%)	
No Load	200	657.10	94.49
	250	43.99	38.24
Full Load	200	95.04	140.11
	250	51.83	124.17

The frequency content in terms of the power spectral density, for the measured shaft signal under normal and rectifier fault condition (no load) is given in Figure 6.1 and Figure

6.2, respectively.

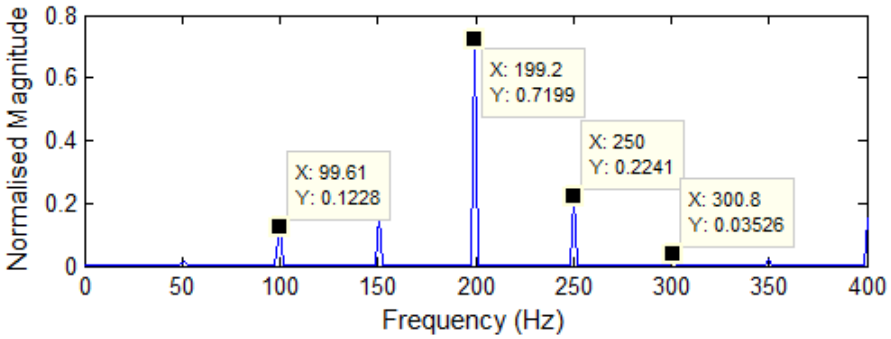


Figure 6.1: Frequency content of power spectral density of shaft voltage without fault

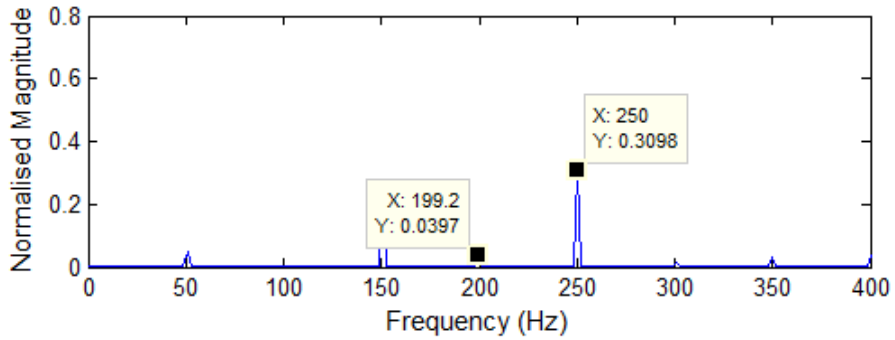


Figure 6.2: Frequency content of power spectral density of shaft voltage with rectifier fault

Changes in the frequency content of each of the signals is explained through analysing the simulated field winding currents for normal and rectifier fault conditions which are shown in Figure 6.3. The simulated field currents are found by viewing the current across the rotor coil elements of the coupling model given in Figure 4.2. Measurement of the field current under normal conditions and rectifier conditions is also carried out using a current probe. The probe measures the flow of current out of the three phase rectifier directly into the field windings (see Appendix C). The graph of the experimental measurements are given in see Figure 6.4.

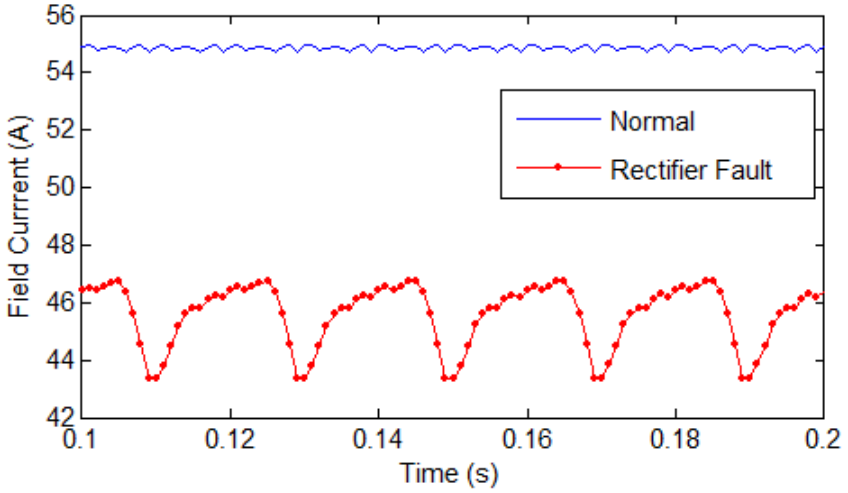


Figure 6.3: Simulated rotor winding current under normal and rectifier fault conditions

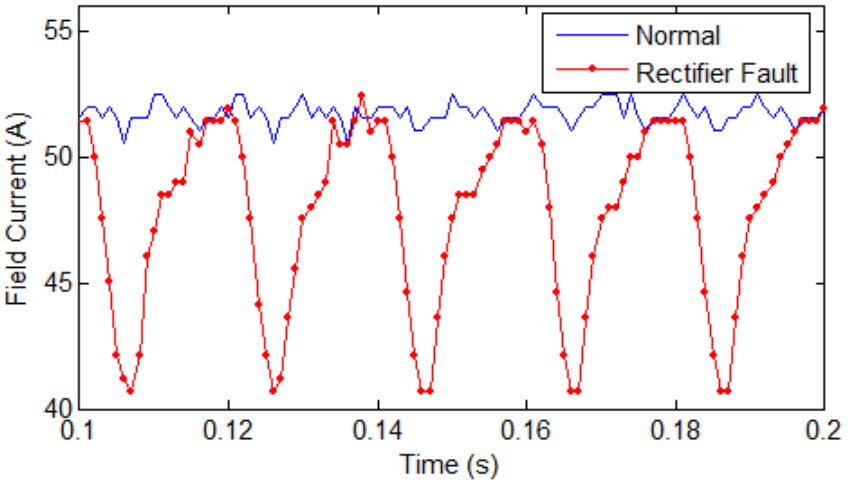


Figure 6.4: Rotor winding current measurement of experimental setup under normal and rectifier fault conditions

6.3 Eccentricity

Similarly, as with the rectifier fault, results for the eccentricity fault is given in Table 6.3 and Table 6.4. It should also be noted that the real machine, under normal conditions, naturally possesses imperfections and some degree of static eccentricity. It is therefore

expected that the harmonic affected by static eccentricity will have some value under normal conditions i.e. i.e. normalised magnitude of 6^{th} harmonic $\neq 0$.

These manufacturing imperfections are transferred to the simulation model in the form of weld recesses and a rotor position error (relative to the stator) of 1.65% i.e. nominal value of 0.099 mm for δ with normal air-gap of 6 mm. The addition of this error to the normal condition simulation model is significant in preventing the percentage change tending towards infinity as the nominal values of the affected harmonics tend to zero i.e. no eccentricity.

Table 6.3: Percentage change in harmonics of flux probe for static eccentricity fault

Condition / δ (mm)		Harmonic (Hz)	Simulation	Measurement
			Percentage change (%)	
No Load	0.5	300	1139.73	34.56
	1.0		2438.72	62.33
Full Load	0.5	300	1689.24	148.91
	1.0		3834.51	359.29

Table 6.4: Percentage change in harmonics of shaft voltage for static eccentricity fault

Condition / δ (mm)		Harmonic (Hz)	Simulation	Measurement
			Percentage change (%)	
No Load	0.5	300	3570.64	26.77
	1.0		8056.62	309.81
Full Load	0.5	300	3457.53	225.68
	1.0		7816.54	570.29

6.4 Short-circuited Excitation Windings

Two turns of the rotor winding are short-circuited as described previously. The results of this fault on specific harmonics are given in Table 6.5 and Table 6.6. The power density

spectra for the measured shaft voltage signal under fault condition is given in Figure 6.5. A considerable increase in the 6^{th} harmonic is evident when compared to the value indicated in Figure 6.1.

Table 6.5: Percentage change in harmonics of flux probe for excitation winding inter-turn short circuit fault

Condition	Harmonic (Hz)	Simulation	Measurement
		Percentage change (%)	
No Load	100	35.53	291.51
	300	123.07	34.54
Full Load	100	35.77	82.80
	300	35.08	64.76

Table 6.6: Percentage change in harmonics of shaft voltage for excitation winding inter-turn short circuit fault

Condition	Harmonic (Hz)	Simulation	Measurement
		Percentage change (%)	
No Load	100	70.1	63.93
	300	888.59	606.108
Full Load	100	61.71	1200.15
	300	241.51	319.12

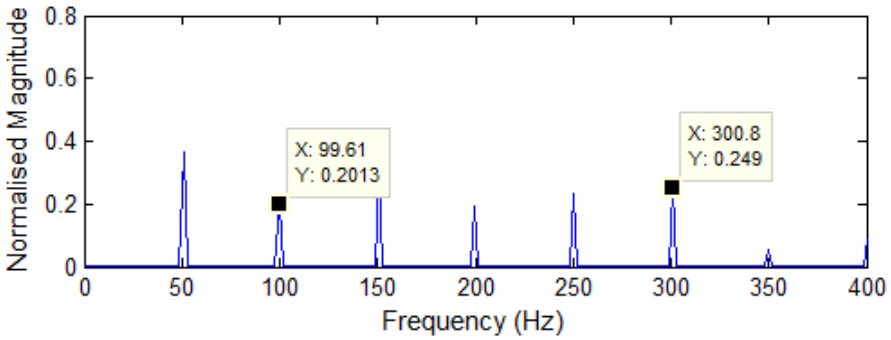


Figure 6.5: Frequency content of power spectral density of shaft voltage with excitation winding fault

6.5 Discussion

Whilst the affected harmonics and extent thereof, varies for each of the presented faults, effects on the actual output waveforms for the flux probe and shaft brushes are insignificant. This is because the investigated faults are incipient faults and usually do not yield a clear indication of presence. The presented methods are intentionally established with the purpose of identifying such faults.

The effects of incipient faults on the output waveforms are expectedly difficult to determine. However, changes in specific harmonics of the power spectra for these waveforms are substantial. Results obtained from a rectifier fault indicate a large degree of influence at 200 Hz and 250 Hz. This is due to the transmission of frequency content of the 50 Hz supply signal through the three phase rectifier to the rotor winding. Translation of the 50 Hz component onto the dynamic rotor winding i.e. 3000 rpm provides the coupling of higher frequency components. Simulations and experimental measurements of the field currents under rectifier fault conditions, shown in Figure 6.3 and Figure 6.4 respectively, indicate the presence of these 50 Hz transients when compared to normal conditions. Additionally, these results verify that a single diode fault is a true incipient fault and cannot be simply diagnosed through a DC measurement i.e. RMS value of the rectifier output under fault condition is approximately equal to the output under normal conditions.

Static eccentricity introduces a considerable change in the 300 Hz component and corresponds to results from previous work [19]. Short-circuited turns on the excitation winding indicate a similar effect on the 6^{th} harmonic and a distinguishable effect at 100 Hz. This is expected as shorted turns on the rotor windings generates a similar asymmetry in the rotating field due to weakened coupling, however it differs moderately from static eccentricity since the asymmetrical field is dynamic.

Numerical inconsistencies between percentage changes in simulated and measured data may be attributed to noise and the influence of peripheral measurement equipment i.e. brushes, dSpace module and other pre-processing components.

Chapter 7

Conclusion

7.1 Outcomes

An investigation into a method for diagnosis of incipient faults on a synchronous generator has been presented. The background to these incipient faults and previous research conducted on fault detection was firstly given. Additionally, the significance of the selected faults to be investigated was provided.

The main objectives of the project were presented as follows:

- Construct a model of miniature 2-pole synchronous generator using a finite element software package.
- Predict behaviour of a generator through simulation of various fault conditions.
- Impose these fault conditions on an actual generator in a controlled environment.
- Measure and analyse the shaft and flux probe signals for each fault condition.

Details of the construction of the model and implementation of each of the fault conditions were given. This was followed by an analysis of the recorded output signals and resulting behaviour of the generator. The experimental aspect of the investigation was optimised through use of simulations as the behaviour of the generator under the specific fault conditions was rendered reasonably predictable.

Results from simulations correlate with the measured data in terms of a definite relationship between each fault and specific harmonics. This implies that specific faults induce distinguishable effects on the frequency content of power spectra for both the flux probe and shaft signals.

The practical implication of the outcomes of this investigation is that incipient faults may be effectively diagnosed through the use of flux probes/search coils and shaft brushes.

7.2 Recommendations for Future Research

Characteristics used to diagnose a fault on a system under multiple fault conditions may not necessarily be the same as for diagnosis of a single fault and investigation of these differences is recommended. The significance of differentiating between faults on a system under multiple fault conditions is that it enables realistic measures for condition monitoring. This is due to the fact that since some faults may cause certain effects that are similar to others and therefore result in a false diagnosis.

An example of this 'shadowing' effect is with rotor winding shorts and eccentricity. A rotor winding short, under static conditions, causes similar disturbances in the magnetic field to rotor eccentricity. In order to definitively diagnose a fault, characteristics and minimal differences between each fault must be also be investigated.

One of the major objectives of the proposed research is to therefore investigate these shadowing effects and any characteristics that may assist in distinguishing between different faults. The results from the investigation are significant in indicating that an inexpensive, reliable, simple and easily implemented fault diagnosis system is achievable.

It is therefore recommended that these results be used to design and implement a fully functional fault diagnosis system. The most significant aspect of the proposed fault diagnosis system will be the algorithm as it will be unique in identifying individual faults. Diagnosis of the extent of the actual fault will have to be considered as this relates to the operational aspect of the algorithm i.e. manner in which algorithm recognises the fault such as look-up table of frequency signatures.

References

[1] S. V. Zyl and C. T. Gaunt, "Control strategies for distributed generators operating on weak distribution networks," *IEEE Powertech Conference, Italy*, 2003.

[2] I. Boldea, "The electric generators handbook: synchronous generators," *Taylor and Francis Group, First Edition*, 2006.

[3] D. de Canha, W. A. Cronje, A. Meyer, and S. J. Hoffe, "Methods for diagnosing static eccentricity in a 2 pole generator," *IEEE Powertech Paper ID 528*, 2007.

[4] E. P. R. I. Corporate, "Generator stator core condition monitoring by tracking shaft voltage and grounding current," *Electric Power Research Institute, California 1020275*, 2010.

[5] G. W. Buckley, R. Corkins, and R. N. Stephens, "The importance of grounding brushes on large turbine generators," *IEEE Transactions on Energy Conversion, Vol. 3, No. 3*, 1988.

[6] S. J. Hoffe, W. A. Cronje, and A. Meyer, "Determination of shaft position from shaft voltage on a synchronous generator," *IEEE International Symposium on Diagnostics for Electric Machines, Power Electronics and Drives - Vienna, Austria*, 2005.

[7] J. Faiz, B. M. Ebrahimi, and M. Valavi, "Mixed eccentricity fault diagnosis in salient-pole synchronous generator using modified winding function method," *Progress In Electromagnetics Research B, Vol. 11*, 2009.

[8] A. Miletic and M. Cettolo, "Experimental research on rotor fault diagnosis using external coil voltage analysis and shaft voltage signal analysis," *International Sym-*

posium on Diagnostics for Electric Machines, Power Electronics and Drives - Vienna, Austria, 2005.

[9] J. Sottile, F. C. Trutt, and A. W. Leedy, "Condition monitoring of brushless three-phase synchronous generators with stator winding or rotor winding deterioration," *IEEE Transactions on Industry Applications, Vol. 42, No. 5*, 2006.

[10] P. I. Nippes, "Early warning of developing problems in rotating machinery as provided by shaft voltages and grounding currents," *IEEE Transactions on Energy Conversion, Vol. 19, No. 2*, 2004.

[11] A. Elez, B. Tomcic, and M. Petrinic, "Detection of inter-coil short circuits in coils of salient pole synchronous generator field winding on the basis of analysis of magnetic field in the machine," *International Conference on Renewable Energies and Power Quality - Granada, Spain*, 2010.

[12] Y. Kim, J. Kim, B. Yoon, S. Lee, and T. Jung, "Detection of shorted-turns in the rotor winding of cylindrical synchronous generators using discrete wavelet transform," *IEEE Applied Power Electronics Conference and Exposition*, 2006.

[13] S. J. Hoffe, "Synchronous generator fault diagnosis using shaft signal measurements," *MSc. Dissertation - University of the Witwatersrand*, 2006.

[14] C. Bruzzese and G. Joksimovic, "Harmonic signatures of static eccentricities in the stator voltages and in the rotor current of no-load salient-pole synchronous generators," *IEEE Transactions on Inustrial Electronics Vol. 58, No. 5*, 2011.

[15] dSpace GmbH, "Controldesk reference guide," *Release 6.5*, 2009.

[16] J. P. A. Bastos, , and N. Sadowski, "Electromagnetic modelling by finite element methods," *Marcel Dekker, First Edition*, 2003.

[17] S. Humphrey, "Finite element methods for electromagnetics," *Taylor and Francis Group, First Edition*, 2010.

[18] C. L. Phillips, J. M. Parr, and E. A. Riskin, "Signals, sytems and transforms," *Prentice Hall, Third Edition*, 2003.

[19] D. de Canha, "Shaft voltage diagnosis of inter-turn field faults in a synchronous generator aided by fem models," *EMF Conference, Brussels*, 2009.

Appendix A

Simulation Model

A.1 Material Characteristics

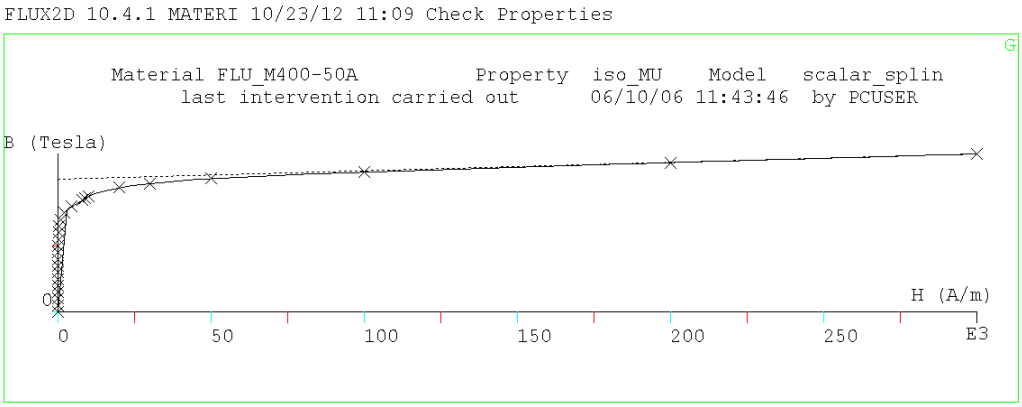


Figure A.1: B-H curve of FLU_M400 steel used for stator core construction in Flux® 10.4.1

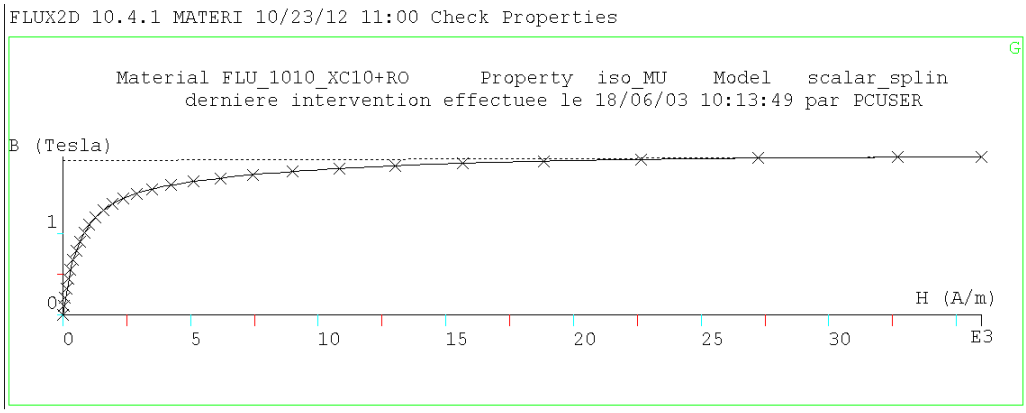


Figure A.2: B-H curve of FLU_1010_XC10 steel used for rotor core and case construction in Flux® 10.4.1

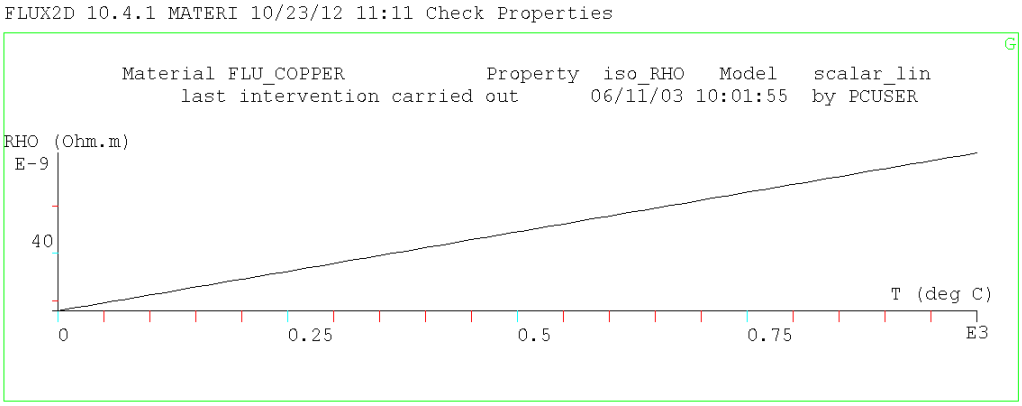


Figure A.3: Resisivity characterisitcs of FLU_copper used for all coil and damper construction in Flux® 10.4.1

Appendix B

Matlab Code

```
%Wesley Doorsamy
%Methods for fault diagnosis on a synchronous 2-pole generator

%Read in data and plot comparison-
%between power spectral density for fault and no fault

fwithout = shaft_NL;
fwith= shaft_NL_WS; %Read in data file



% for k=1:length(fwith)
% fwith(k)=fwith(k)/100;
% fwithout(k)=fwithout(k)/100;
% end %Perform normalisation if required

ansy = fwithout;
ansy1 = fwith; %Declare some structures

Y = fft(ansy,512);
Pyy = Y.* conj(Y) / 512;
f = 1000*(0:256)/512; %Perform FFT and calc PSD

Y1 = fft(ansy1,512);
Pyy1 = Y1.* conj(Y1) / 512; f = 1000*(0:256)/512; %Perform FFT and calc PSD

subplot(2,1,1); plot(f,Pyy1(1:257))
subplot(2,1,2);plot(f,Pyy(1:257)) %Plot results
title('Frequency content of y') xlabel('frequency (Hz)')
```

Appendix C

Instrumentation

C.1 Current Probe



Figure C.1: Current probe used to measure three-phase rectifier output to field windings on rotor

C.2 Peripherals



Figure C.2: Amplifier used with current probe to measure three-phase rectifier output to field windings on rotor



Figure C.3: BNC termination (feedthrough) used to connect amplifier to DSpace controller panel

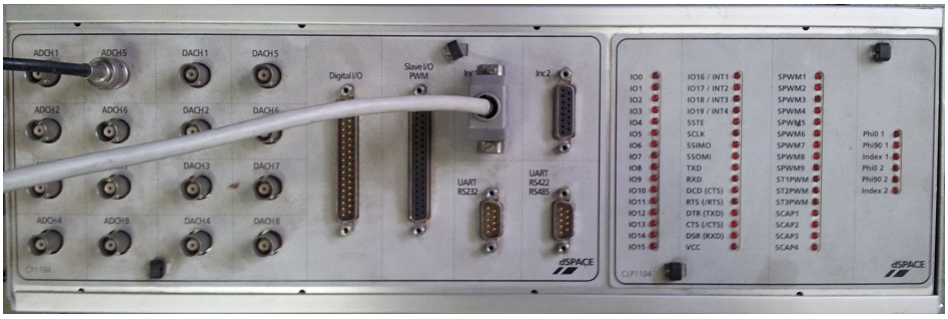


Figure C.4: CLP1104 controller panel used to interface with dSpace card and workstation